Ultra-Low Power, Low Voltage, Autonomous Resonant DC-DC Converter for Wireless Sensors

Salah-Eddine Adami, Nicolas Degrenne, Christian Vollaire, Bruno Allard, Francois Costa

▶ **To cite this version:**

Salah-Eddine Adami, Nicolas Degrenne, Christian Vollaire, Bruno Allard, Francois Costa. Ultra-Low Power, Low Voltage, Autonomous Resonant DC-DC Converter for Wireless Sensors. 4th IEEE POWERENG, May 2013, Istanbul, Turkey. 10.1109/PowerEng.2013.6635787 . hal-01736241

HAL Id: hal-01736241
https://hal.science/hal-01736241v1

Submitted on 16 Mar 2018

HAL is a multi-disciplinary open access archive for the deposit and dissemination of scientific research documents, whether they are published or not. The documents may come from teaching and research institutions in France or abroad, or from public or private research centers.

L'archive ouverte pluridisciplinaire **HAL**, est destinée au dépôt et à la diffusion de documents scientifiques de niveau recherche, publiés ou non, émanant des établissements d'enseignement et de recherche français ou étrangers, des laboratoires publics ou privés.

Ultra-Low Power, Low Voltage, Autonomous Resonant DC-DC Converter for Wireless Sensors

Salah-Eddine Adami, Nicolas Degrenne, Christian Vollaire, Bruno Allard
University of Lyon, Ecole Centrale de Lyon
Ampere Laboratory
Lyon, France
salah-eddine.adami@ec-lyon.fr

François Costa
University Paris Est Créteil
SATIE Lab, ENS de Cachan
Cachan, France

***Abstract*—This article presents a resonant DC-DC converter topology suitable for ultra-low power and low voltage applications. The presented topology is dedicated to energy harvesting sources in general and especially for Radio-Frequency RF sources. Main advantage of this converter is its autonomy, i.e., it operates from low voltage levels without the need of an external energy source or any other startup assistances. Theoretical modelling of the converter is used together with circuit simulations in order to make an optimal design based on the requirements of a low power rectifying antenna (rectenna). A discrete prototype was fabricated and tested. Low voltage and ultra-low power as lows as 100mV and 3.7µW respectively were achieved. The input low voltage is boosted to a usable over 1Volt level allowing to power wirelessly and autonomously low power circuits as wireless sensors.**

Keywords- ultra-low power, low voltage, resonant DC-DC converter, RF energy harvesting, rectenna.

I. INTRODUCTION

Wireless sensors networks (WSNs) [1] are nowadays ubiquitous in various kinds of applications like: monitoring and control, smart building, healthcare, etc. The expansion of WSNs is due, among other reasons, to the efforts made by designers in order to develop low-power circuits. Though those circuits are optimized for low power and have excellent power consumption budget, the problem of autonomy is still there. In fact, the performances required from an autonomous sensor grow day by day and it is likewise for the power consumption. In most applications, batteries are used alone in order to supply WSN nodes. In this case, the sensor life-time is limited. So, designers introduce energy harvesting as a support together with batteries. Harvested energy could be used to recharge the batteries or/and to power directly the sensors.

In most cases, energy-harvesting sources deliver very low voltage level (<1V). However, a level of some volts is needed in order to be able to supply conventional circuits as autonomous sensors. A power management system based on step-up DC-DC converter is used for this purpose. But again, the converter control circuit needs a power supply in order to operate. There are two possibilities in order to initiate the converter operation: a first solution is to use external start-up assistance; a second one is to use a low voltage start-up circuit. In the first case, there are three possibilities; an external battery, a precharged capacitor or mechanical switch.

A Battery-based start-up aid is the most frequently used technique due to its simplicity. In [2] a DC-DC boost converter for low power RF energy harvesting (from 10µW) is presented; the output rechargeable battery is used to store the harvested energy and also to initiate and supply the converter control circuit. However, batteries have limited charge/discharge cycles, and the initial performances somewhat degrade with time. In addition, batteries are space consuming and they take large amount of the global sensor area. Furthermore, sensors could be exposed to critical conditions like: extreme temperature, chemical medium, etc. In this case batteries usage becomes critical.

In some specific applications, a factory-precharged capacitor is used. The stored energy allows the converter to start-up. Thereafter, the start-up capacitor is recharged by the energy-harvesting source for other future usages. In [3] a boost inductive DC-DC converter harvests thermal energy from a low voltage thermoelectric generator (TEG, from 20mV). The output capacitor should be precharged to at least 650mV in order to guarantee the converter start-up. The main advantage of such a technique is that it avoids the use of a battery. However, if the circuit is not used for a certain time, the stored energy will be lost due to capacitor leakage currents.

If there is a mechanical vibration source, a small scale MEMS piezoelectric device could be used. For example [4] presents a power management system for thermal energy harvesting; a mechanical switch is used that allows the principal boost converter to start-up from 20mV of input voltage without external battery assistance.

An autonomous architecture avoids the use of any external start-up assistance (battery, precharged capacitor or mechanical switch). In this case of autonomous operation, a start-up circuit is used. The start-up circuit is a special low-power and low-voltage DC-DC converter. Due to its poor performances (no regulation and poor efficiency in general), such a circuit is only used during the transient phase. Once the output reaches a convenient voltage level, the start-up circuit is disabled and during the steady-state phase, the principal converter control circuit is only powered by the output. Nonetheless, in some

cases, the available power is not sufficient; the start-up circuit is used alone. Start-up circuits can take two forms: a switched capacitor converter or a resonant converter.

Special low voltage switched capacitor converters are widely used in sub-1 volt applications [5]. In fact, the architecture of the converter is optimized for low voltage operation. In addition, different techniques are used to reduce the MOSFETs' threshold voltages as: Silicon-On-Insulator (SOI) technology [6], forward body biasing [7], threshold voltage programming by charge injection [8]. The input voltage can be reduced to near 300mV [5] or even lower [9] (however, stability problems are reported). In addition, switched capacitor converters could be integrated easily, enabling self-starting capability in small-scale applications. However, a significant input current is necessary [5], what limits the possible use at medium current level (from 1mA).

The second category of self-powered converters uses resonant DC-DC converters. The Armstrong oscillator [10–14] is commonly used in this field. The major benefit is the ultra-low input voltage and also high-voltage stepping-up abilities. Resonant circuits may also be used as a start-up part of a principal converter. Most resonant circuits operate at milli-watts output power levels. In [10] a 100mW boost converter using the Armstrong oscillator as a start-up stage is presented. Similar topologies are presented in [13] and [14] for 10mW and 1mW respectively.

Fig. 1 shows a summary of the state-of-the-art of low-power and low-voltage DC-DC converters classified with respect to start-up techniques. It can be observed that converters using external start-up assistance cover all voltage-power ranges (battery [2], [15], precharged capacitor [16], [17], mechanical switch [18]). Self-starting converters based on switched capacitors are used from 200mV and 1mW of source voltage and power respectively [5]. Classical resonant converters cover ultra-low input voltage (from 20mV) and low-power (from 1mW) ranges [10–14]. The proposed resonant converter fills the white area in the diagram of self-starting converter that corresponds to a low input voltage (from 100mV) and ultra-low power (from some µW) ranges.

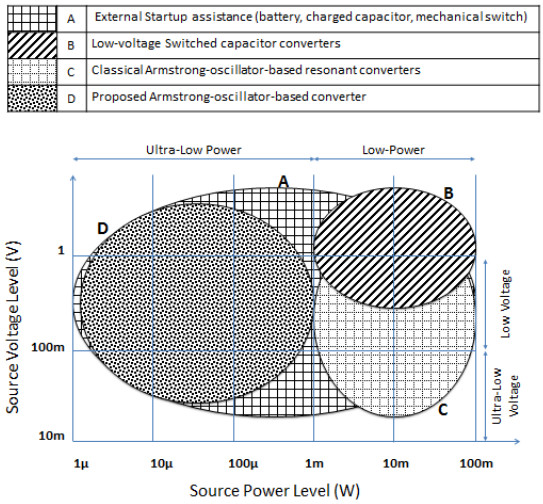

Figure 1. State of the art of low voltage and low power converters

The objective of this article is to present a resonant converter suitable for ultra-low power and low voltage applications. The motivation is the self-operation needs in ultra-low power energy harvesting sources. Such sources are generally characterized by a high internal impedance, what is the case for RF energy harvesting for example. The following section will introduce the considered RF energy harvesting source. In section III, the proposed resonant converter is presented as well as its theoretical modeling. Experimental tests are presented in section IV concerning a discrete prototype and low RF energy to be harvested.

II. LOW-POWER RECTENNA

The association of a receiving antenna and an RF-DC rectifier circuit is called a rectenna (rectifying antenna). A rectenna usually operates in the range of UHF (f > 1GHz) enabling long range wireless energy transfer with relatively compact antennas.

Rectenna operation principle is illustrated in Fig. 2. The incident RF power is captured by an antenna under the form of a high frequency sine wave. This is then transformed into DC power by the diode-based converter. A HF filter ensures impedance adaptation between the antenna and the diode rectifier around work-frequency (2.45GHz) for optimal power transfer. The output DC filter smooths the output DC voltage and current by attenuating high frequency harmonics present in the RF signal or generated by the rectification process itself.

In the case of low incident power levels (below 1mW), rectifier is often based on series-mounted diode. This structure offers the best compromise between DC output voltage level and conversion efficiency at those low incident power levels [18]. Furthermore, zero bias Schottky diodes are often used in this case due to their low threshold voltage (around 150 mV) and their low junction capacitance (0.18 pF) [19].

A prototype of a single series-mounted diode rectenna was fabricated on a low-cost 1.6 mm FR4 substrate. In order to evaluate the rectenna output characteristic, the fabricated prototype was tested under wide range of input RF power and output load resistance. RF power is directly supplied by a power source through a SMA cable. Current-Voltage (I-V) and Efficiency-Load (η-R) characteristics are shown in Fig. 3.

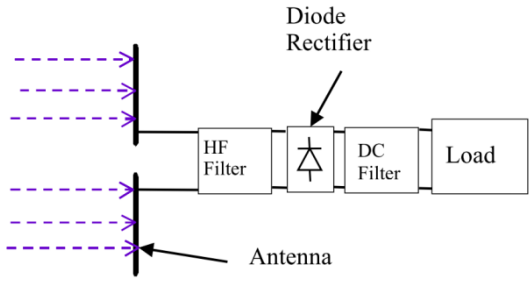

Figure 2. Block diagram of a rectenna circuit

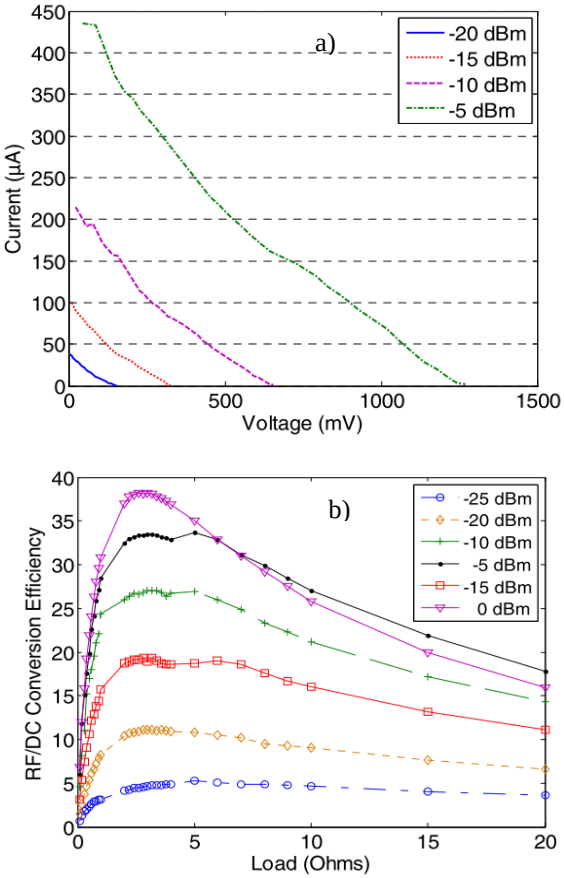

Figure 3. Series-mounted rectenna output characteristic: a) Current-Voltage, b) Efficiency-Load

I-V characteristic are almost parallel straight lines. In addition, conversion efficiency is maximal for a specific fixed output load value. Therefore, rectenna output DC model is a voltage source in series with its internal impedance. This internal impedance is equal to the optimal load value (2.4kΩ in this case). For a -15dBm (30μW) level of injected RF power, output open-circuit voltage is equal to 300mV. In this case, the maximum DC power is around 10μW. In order to be able to use this energy, a specific DC-DC converter topology would be needed in order to provide a conventional over 1V voltage level.

III. Resonant DC-DC Converter Topology and Design Methodology

A resonant converter is a type of DC-DC converter that operates with self-oscillation and self-control modes. In fact, no additional control circuitry nor external energy source are required for a proper operation. In addition, thanks to its inherent voltage step-up topology, the input voltage level can be very low.

A. Topology and operation

Fig. 4 depicts the converter topology and main operational blocs. The resonant converter is composed by two main components: a high turn-ratio transformer and a normally-on N-channel JFET (in order to guaranty the self-starting mode).

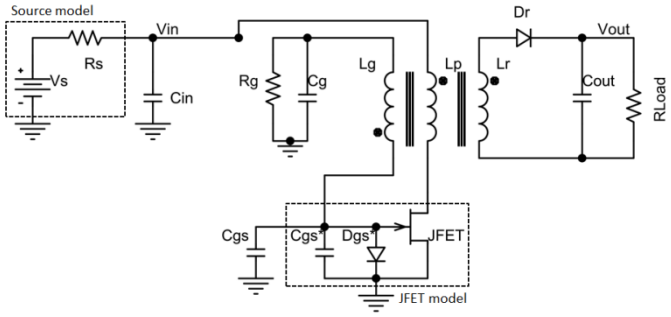

Figure 4. Resonant converter topology

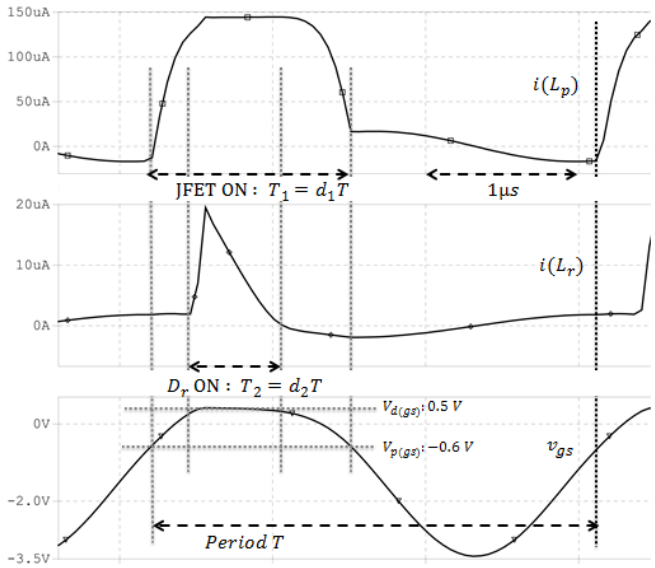

Figure 5. Steady state imulated waveforms for $V_s = 200mV, R_s = 1k\Omega$ *and* $R_{load} = 1M\Omega$: primary inductance current $i(L_p)$, tertiary inductance current $i(L_r)$ and JFET's gate-source voltage v_{gs}

The operation of the converter is based on three functional blocks. The first functional block is the oscillator. It is formed, on the one side, by the transformer and the gate-source capacitance C_{gs} (resonant cavity) and on the other side, by the JFET (negative gain amplifier). The oscillation frequency is fixed by the transformer secondary inductance ($L_g = {m_g}^2 L_p$) and the gate-source capacitance (C_{gs}). The latter capacitance is composed of a real capacitor, the JFET gate-source capacitance, the other JFET parasitic capacitances and the transformer stray capacitances.

Fig. 5 shows the JFET gate voltage waveform v_{gs}. It can be seen that the positive side (during the JFET on-phase) is clamped (to $V_{d(gs)}$ = 0.6V) by the JFET's inherent gate-source diode. In the negative side (during the JFET off-phase), the waveform has a sinusoidal form and a high peak level with respect to the input voltage.

The second function is a voltage step-up that is possible thanks to the transformer high turn-ratio. A high voltage level is needed at JFET's gate level in order to reach the channel cut-off voltage and then switch it on and off. Also, high voltage is

needed at tertiary winding level ($L_r = {m_r}^2 L_p$) in order to obtain a high DC voltage at the output.

The third functional block is the rectifier which is done using the rectification diode D_r. As it can be observed from waveforms on Fig. 4, D_r is on when JFET's channel and D_{gs} are on. The capacitor C_g is charged negatively when D_{gs} become on and it allows obtaining a high voltage level at JFET's gate level. A high resistor value (R_g) is placed in parallel with C_g in order to stabilize the voltage across this capacitor.

B. Converter modelling and design methodology

The resonant converter is a self-controlled converter. Therefore, all performances (minimal input voltage and current levels, efficiency, output voltage, oscillations frequency) are predetermined by the converter components. In order to determine the impact of the converter parameters on performances and also existing trades-offs, a global model is considered. The first part focuses on the converter oscillation start-up conditions and the second one on the steady-state mode.

1) Startup conditions

The resonant converter includes an Armstrong oscillator structure. As every harmonic oscillator, there are some conditions that guaranty the oscillation start-up. Those conditions depend on the elements that compose the oscillator and also on the external conditions, like the input power source model. So, the converter and the energy source are modeled during transient phase. During this phase, the following hypotheses are considering:

- The source model is a DC voltage source V_s in series with its internal impedance R_s.
- A perfect coupling between primary and secondary windings is considered (coupling coefficient k =1).
- The winding equivalent resistances are negligible with respect to R_s and magnetic losses are negligible.
- As the input voltage is very low ($< 1V$), the drain-source JFET voltage (v_{ds}) is consequently very-low. The JFET is supposed to operate only in the linear (or triode) region.
- v_{gs} never reaches $V_{d(gs)}$. Therefore, D_{gs} is off and does not impact on the transient mode. The same for D_r which is off during the startup phase.

The expression of the JFET drain-source current i_{ds} in the triode region is given as function of v_{gs} and v_{ds} by:

$$i_{ds}(v_{gs}, v_{ds}) = \frac{2I_{DSS}}{{V_p}^2}\left(v_{gs} - V_p - {v_{ds}}/{2}\right).v_{ds} \quad (1)$$

I_{DSS} is the zero gate-voltage drain current and V_p is the gate-source cutoff voltage. Using this expression and previously announced hypothesizes, a second-order nonlinear differential equation for v_{gs} is obtained. At the best known of authors, no analytical solution can be found for such an equation. However, our purpose is to find the oscillation conditions. Those conditions can be found by considering the instability conditions of the system, i.e. a negative value for the reduced-determinant Δ' (oscillating system) and a negative value of the damping factor λ (divergent oscillations). The expressions of Δ' and λ still contain variable quantities. Nevertheless, if we observe the circuit at a moment very close to the start-up, then we can consider that v_{gs} is near zero. Finally, two oscillation conditions are found:

$$V_{s\,min} = \frac{2I_{DSS}R_s + |V_p|}{m_g} \quad (2)$$

$$m > \frac{1}{\left(\frac{V_s}{2I_{DSS}R_s - V_p}\right) - \sqrt{\frac{C_{gs}}{L}}\left(\frac{2I_{DSS}R_s - V_p}{I_{DSS}}\right)} \quad (3)$$

The expression in (2) is a very important result for the converter design. In fact, it gives the minimal source open-circuit voltage ($V_{s\,min}$) needed in order to satisfy the oscillator start-up conditions. $V_{s\,min}$ depends on the source internal impedance, R_s, the JFET parameters (I_{DSS} and V_p) and the transformer turn-ratio m_g. The latter value has a high value for such kind of applications ($m \gg 1$).

Besides, the turn-ratio m has a minimal value that guaranties oscillation start-up. Furthermore, increasing the turn ratio over the latter minimal value will lead to obtain smaller values for V_s. In fact, a high value of *m* provides high voltage oscillations, allowing JFET commutations even if the input voltage is low. Nevertheless, a large value of m will result in a large secondary inductance and then a bulky transformer.

2) Steady-state modeling and analysis

This part gives a study of the steady-state phase, i.e. when the output voltage reaches its final value. It can be considered that during steady-state, the switches (JFET channel and diodes) are considered as ideal, i.e. they have only two possible states: on or off.

A period is divided into different phases with respect to the states of the switches. A classical approach is used here, i.e. an equivalent circuit for each phase is derived and relative differential equations are computed. Using initial conditions for each phase, analytical expressions of voltages, currents and phases' durations are derived. We assume that the JFET's channel and D_r are on during $T_1 = d_1 T$ and $T_2 = d_2 T$ respectively (see Fig. 5).

From the circuit schematic (Fig. 4), it can be noticed that when JFET's channel and D_r are both on the converter's output voltage is equal to the input one multiplied by m_r. In addition, during steady-state, V_{in} as well as V_{out} are considered as constant during all the operation period. This expression is therefore valid for the all operation period. However, it is more interesting to find a relation using the source open circuit voltage V_s rather then V_{in}.

A theoretical expression of the voltage step-up ratio can be found by making an overall balance of power for a complete operation period. If we assume that the converter is lossless, the power delivered by the source is consumed at output load level. This hypothesis leads to obtain the following expression:

$$\frac{V_{out}}{V_s} = \frac{m_r}{{m_g}^2 \frac{R_s}{R_{out}} + 1} \quad (4)$$

IV. EXPERIMENTAL TESTS

A. Prototype design

In this part, the objective is to give a resonant converter design example based on specific source requirements and using previous analytical equations and circuit simulations. In fact, the designed converter should interface a high internal impedance rectenna ($R_s = 2.4k\Omega$) and guaranty start-up for some hundreds of mV (from 300mV) of source input voltage level. The output voltage level should be over 1V and the efficiency as good as possible.

A discrete prototype was fabricated. Regarding to optimization process, the best commercially available JFET is the device J201 (I_{DSS}=583µA; V_p=-0.6V). Low I_{DSS} and low V_p allows obtaining a small startup voltage. However, this will increase steady-state losses. Tertiary winding rectification diode is the HSMS2822 which was chosen thanks to its low forward voltage ($V_f = 340mV$) allowing then to minimize conduction losses. The three winding transformer ($L_p = 50\mu H$; $m_g = 25$; $m_r = 25$) was realized using a compact (20mm x 10mm x 6mm) and high frequency (up to 600kHz) E ferrite core in order to obtain a compact structure which is suitable for embedded and portable applications (like WSNs). Beside the transformer dimensions are very small as regard to the source's one (antenna and rectifier), future works will consider to optimize the transformer sizing in order to obtain dimensions in the mm order which is realizable because the power and the current levels are ultra-low.

B. Tests using a rectenna model

The first step of experimental tests was achieved using a rectenna emulation model, i.e. a programmable low-voltage source with an additional series-mounted high resistor in order to model the rectenna internal impedance.

Fig. 6 shows the converter output voltage versus the input one. The converter minimum startup voltage is 100mV (200mV for source open circuit voltage V_s) which correspond to a power level as low as 4µW. Voltage step-up ratio is near to what it was expected from theoretical calculations (equation (4)), i.e. an average value of 10 which is in addition, quiet stable over all input voltage range.

Fig. 7 shows the experimental efficiency for two load resistance values. The power efficiency is calculated using the voltage source level (V_s), the internal resistance (R_s), the converter input voltage (V_{in}), the converter output voltage (V_{out}) and the load resistance (R_{out}):

$$\eta = \frac{P_{out}}{P_{in}} = \frac{\frac{V_{out}^2}{R_{out}}}{(\frac{V_s - V_{in}}{R_s})V_{in}} \quad (5)$$

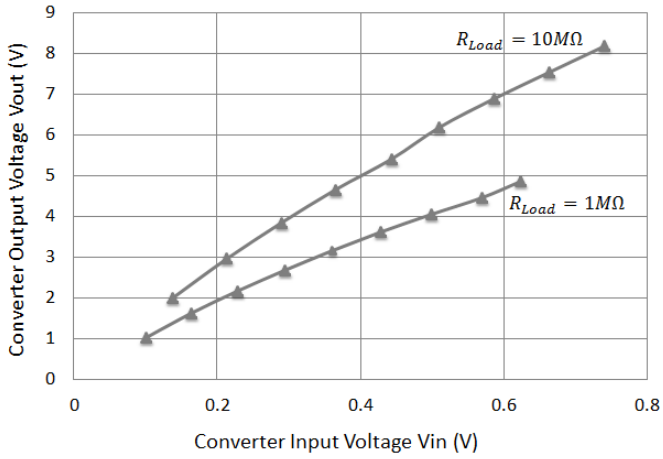

Figure 6. DC-DC converter input and output voltages

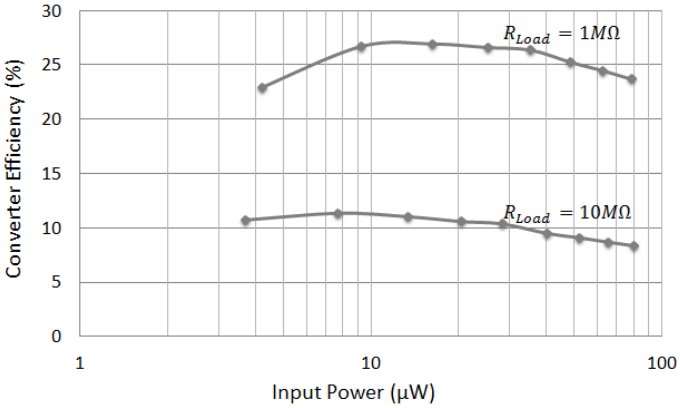

Figure 7. DC-DC converter efficiency vs. input power

The efficiency is around 25% and 10% for 1MΩ and 10 MΩ of load resistance values respectively. Losses are concentrated in the JFET's channel resistance. As it was shown previously in section III, a minimum source startup voltage is achieved using a low I_{DSS} JFET device (Equation (2)), i.e., a high channel resistance. There is then a trade-off between startup capability and steady-state efficiency.

One of the most interesting applications of such a converter is to use it as a startup circuit for a principal controlled standard converter. In this case, the resonant converter will be used in the transient phase in order to charge a capacitor with a sufficient voltage level, next this energy allows to power the control circuitry of the principal converter and the resonant one is disabled.

Several commercially low-voltage, low-power self-starting integrated DC-DC converters (TI bq25504 [24], Cymbet CBC915-ACA [25], ALD300 [26]) were tested in order to make a performance comparison. Due to the extreme low available current level, no one of the converters started-up, even for voltage levels over 300mV.

C. Tests using real rectenna

In this part, a resonant converter is tested using a real rectenna in order to harvest RF energy. The rectenna used her is a low-power rectenna with a 3.9kΩ of internal impedance.

The RF power is injected at the input of the rectifier using a RF power source (at 2.36 GHz). The resonant converter is connected to the rectenna's output and a resistive load (1MΩ) is placed at its output. The input RF power is swept from -16dBm to 0dBm. Fig. 8 shows the converter input and output voltages and the voltage step-up ratio. While the input voltage is almost always under 1V level, the output one grows to near 8V for 0dBm. The step-up ratio varies from 5 to 10.

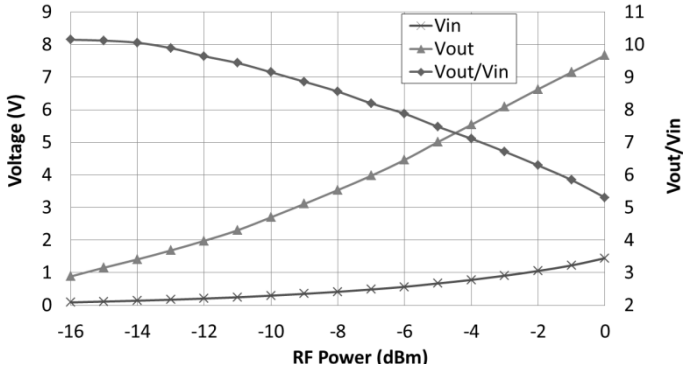

Figure 8. The converter powered by a rectenna: converter input and output voltages Vs. rectenna input power

V. CONCLUSION

Thanks to this resonant converter topology, ultra-low power (as low as 3.7µW) and low voltage (100mV) rectennas can be used in order to provide a completely autonomous wireless power source in WSN applications. In such applications, low RF energy could be either the ambient energy (assuming to be not far from the emitter) or a voluntary RF source. In the two previous cases, the emitter power is limited by the standards in order to avoid EMI and health problematics.

The presented converter can be used either as a principal converter in ultra-low power applications or as a startup bloc for a principal controlled converter. In this case, although the resonant converter overcomes the problematic of autonomous low voltage operation, a sufficient power level is essential in order to be able to power the control circuitry of the principal converter and then to have a positive energy transfer.

Although it was designed and optimized for rectennas, the presented topology can be used for the others energy harvesting sources with similar characteristics as: thermal, microbial fuel cells and mechanical vibrations sources.

ACKNOWLEDGMENT

This work was supported by the ANR (Agence National de la Recherche) through the project REC-EM ANR-10-BLAN-0906

REFERENCE

[1] C. O. Mathúna, T. O'Donnell, R. V. Martinez-Catala, J. Rohan, and B. O'Flynn, "Energy scavenging for long-term deployable wireless sensor networks.," Talanta, vol. 75, no. 3, pp. 613–23, May 2008.

[2] T. Paing, J. Shin, R. Zane, and Z. Popovic, "Resistor Emulation Approach to Low-Power RF Energy Harvesting," IEEE Transactions on Power Electronics, vol. 23, no. 3, pp. 1494–1501, May 2008.

[3] E. J. Carlson, K. Strunz, and B. P. Otis, "A 20 mV Input Boost Converter With Efficient Digital Control for Thermoelectric Energy Harvesting," IEEE Journal of Solid State Circuits, vol. 45, no. 4, pp. 741–750, 2010.

[4] Y. K. Ramadass and A. P. Chandrakasan, "A Battery-Less Thermoelectric Energy Harvesting Interface Circuit With 35 mV Startup Voltage," IEEE Journal of Solid-State Circuits, vol. 46, no. 1, pp. 333–341, Jan. 2011.

[5] Seiko, "S-882Z Ultra-low voltage operation charge pump IC for step-up DC- DC converter startup," Datasheet, 2010.

[6] Y. Yoshida, F. Utsunomiya, and T. Douseki1, "Adaptive-Vth CMOS/SOI DC-DC Converter Scheme for 0.3-V Operation," in 2006 IEEE international SOI Conferencee Proceedings, 2006, pp. 119–120.

[7] P. Chen, K. Ishida, X. Zhang, Y. Okuma, Y. Ryu, M. Takamiya, and T. Sakurai, "0.18-V Input Charge Pump with Forward Body Bias to Startup," IEEE Transactions On Electronic Computers, vol. E94-C, no. 4, pp. 598–604, 2011.

[8] P.-H. Chen, K. Ishida, K. Ikeuchi, X. Zhang, K. Honda, Y. Okuma, Y. Ryu, M. Takamiya, and T. Sakurai, "A 95mV-startup step-up converter with Vth-tuned oscillator by fixed-charge programming and capacitor pass-on scheme," in IEEE International Solid-State Circuits Conference, 2011, pp. 216–218.

[9] P.-H. Chen, K. Ishida, X. Zhang, Y. Okuma, Y. Ryu, M. Takamiya, and T. Sakurai, "A 80-mV input, fast startup dual-mode boost converter with charge-pumped pulse generator for energy harvesting," in IEEE Asian Solid-State Circuits Conference, 2011, pp. 33–36.

[10] J. M. Damaschke, "Design of a low-input-voltage converter for thermoelectric generator," IEEE Transactions on Industry Applications, vol. 33, no. 5, pp. 1203–1207, 1997.

[11] M. Pollak, L. Mateu, and P. Spies, "Step-up DC-DC-Converter with coupled inductors for low input voltages," Fraunhofer IIS, 2008.

[12] L. Mateu, M. Pollak, and P. Spies, "Analog Maximum Power Point Circuit Applied to Thermogenerators," iis.fraunhofer.de. PowerMEMs, pp. 1–4.

[13] N. Degrenne, B. Allard, F. Buret, S.-E. Adami, D. Labrousse, C. Vollaire, and F. Morel, "A 140 mV Self-Starting 10 mW DC/DC Converter for Powering Low-Power Electronic Devices from Low-Voltage Microbial Fuel Cells," Journal of Low Power Electronics, vol. 8, no. 4, p. 13, 2012.

[14] M. Pollak, L. Mateu, and P. Spies, "DC-DC Converter With Input Polarity Detector For Thermogenerators," in PowerMEMS, 2009, pp. 419–422.

[15] A. Dolgov, R. Zane, and Z. Popovic, "Power Management System for Online Low Power RF Energy Harvesting Optimization," Ieee Trans Circuit Syst I, vol. 57, no. 7, pp. 1802–1811, 2010.

[16] E. Carlson and K. Strunz, "20mV input boost converter for thermoelectric energy harvesting," VLSI Circuits, 2009 Symposium, vol. 2, pp. 162–163, 2009.

[17] C. Himes, E. Carlson, R. J. Ricchiuti, B. P. Otis, and B. A. Parviz, "Ultra-Low Voltage Nanoelectronics Powered Directly , and Solely , from a Tree," Journal of Nano, pp. 1–3, 2009.

[18] Y. K. Ramadass and A. P. Chandrakasan, "A Battery-Less Thermoelectric Energy Harvesting Interface Circuit With 35 mV Startup Voltage," IEEE Journal of Solid-State Circuits, vol. 46, no. 1, pp. 333–341, Jan. 2011.

[19] V. Marian, C. Vollaire, J. Verdier, and B. Allard, "Potentials of an Adaptive Rectenna Circuit," IEEE Antennas and Wireless Propagation Letters, vol. 10, pp. 1393–1396, 2011.

[20] B. Merabet, F. Costa, H. Takhedmit, C. Vollaire, B. Allard, L. Cirio, and O. Picon, "A 2.45-GHz localized elements rectenna," in 2009 3rd IEEE International Symposium on Microwave, Antenna, Propagation and EMC Technologies for Wireless Communications, 2009, pp. 419–422.

[21] T. Instruments, "bq25504 Ultra Low Power Boost Converter with Battery Management for Energy Harvester Applications," Datasheet, 2011.

[22] C. Corporation, "Cymbet CBC915 EnerChip TM Energy Processor for Energy Harvesting Applications," Datasheet, 2012.

[23] A. L. D. Inc., "EH300/EH301 EPAD Energy Harvesting Modules for low power applications," Datasheet, 2007.